Purification and characterization of rat hippocampal CA3-dendritic spines associated with mossy fiber terminals

Michael A. Kiebler[a],*, Juan Carlos López-García[b], Philip L. Leopold[c]

[a]*EMBL, Cell Biology Programme, Meyerhofstr. 1, 69117 Heidelberg, Germany*
[b]*Instituto Cajal (CSIC), Madrid, Spain*
[c]*Departments of Medicine and Biochemistry, Cornell University Medical College, New York, NY, USA*

Abstract We report a revised and improved isolation procedure for CA3-dendritic spines, most of them still in association with mossy fiber terminals resulting in a 7.5-fold enrichment over nuclei and a 29-fold enrichment over myelin. Additionally, red blood cells, medullated fibers, mitochondria and small synaptosomes were significantly depleted. We show by high resolution electron microscopy that this subcellular fraction contains numerous dendritic spines with a rich ultrastructure, e.g. an intact spine apparatus, membranous organelles, free and membrane-bound polyribosomes, endocytic structures and mitochondria. This improved experimental system will allow us to study aspects of post-synaptic functions at the biochemical and molecular level.
© 1999 Federation of European Biochemical Societies.

Key words: Dendritic spine; Mossy fiber; Hippocampus; Nitric oxide synthase; Electron microscopy

1. Introduction

Despite the obvious importance of dendritic spines (DS) [1], there is no well established biochemical in vitro system (e.g. synaptosomes [2]) available to allow a thorough analysis of this neuronal compartment. The closest biochemical correlate represents preparations containing pre-synaptic endings in contact with larger membrane-bound sacs with associated post-synaptic densities (PSD). These were named mossy fiber (MF) synaptosomes, synaptoneurosomes, synaptodendrosomes or microsacs [3–7]. However, a subcellular fractionation has not yet been reported for most of these structures with the exception of MF synaptosomes. This purification scheme [6,7] has been developed for the purification of MF terminals. However, this crude preparation still contained significant (nuclear) contamination and has not yet been analyzed for the presence of dendritic spines by applying morphological or functional criteria. Nevertheless, such a preparation has been used to assay the dendritic localization of mRNAs [8,9] or the regulation of local protein synthesis in dendrites [10,11].

In the present study we report on a revised purification procedure for MF synaptosomes which we reanalyzed for the presence of CA3-DS still in association with MF terminals. We improve the procedure by adding a velocity flotation

---

*Corresponding author. Fax: (49) (7071) 601 305.
E-mail: Michael.Kiebler@tuebingen.mpg.de

of the starting material to deplete for red blood cells, medullated fibers, myelin, mitochondria, nuclei, and small synaptosomes. The isolated CA3-DS associated with MF terminals are further analyzed morphologically by high resolution electron microscopy (EM). Finally we propose a functional assay based on the post-synaptic nitric oxide synthase (NOS) to test for the functional integrity of DS.

2. Materials and methods

2.1. Isolation of dendritic spines

15–40 young adult Sprague-Dawley rats (5–7 weeks old: Hilltop Lab Animals, Scottdale, PA, USA) were used per experiment and killed by asphyxiation with CO_2 and decapitation according to the guidelines of the IACUC. Brains were washed with ice-cold homogenization buffer (HB), rapidly dissected and hippocampi stored in ice-cold HB. Hippocampal tissue was manually homogenized and stored in HB (including Mg^{2+} to stabilize large membrane structures) using a glass-teflon Dounce-type homogenizer (clearance: 0.25 mm, VWR, South Plainfield, NJ, USA) as described by Terrian et al. [6]. Upon completion of dissection, a second manual homogenization was performed using a glass-teflon Dounce-type homogenizer (clearance: 0.15 mm, VWR), the material was filtered through a series of nylon filters (100, 74 and 53 μm) to remove larger aggregates and blood vessels and centrifuged at $900 \times g$ for 10 min at 4°C. The resulting pellet was washed, re-sedimented, carefully resuspended in 0.25 volume of HB and adjusted to 25% Optiprep (Gibco BRL, Life Technologies GmbH, Eggenstein, Germany) with a 50% Optiprep working solution as recommended by the supplier. Then, 8.0 ml of the 25% Optiprep/P_1-pellet solution was loaded at the bottom of a 25.5 ml step gradient (9, 12.5 and 15% Optiprep solution in HB) in a SW28 Ultra-Clear centrifuge tube (Beckman Instruments, Munich, Germany) with a long steel syringe needle and centrifuged in a SW28 Beckman ultracentrifuge: 10 000 rpm, 1.32×10^9 ω^2t at 4°C (approximately 20 min). A typical gradient (Fig. 1) yielded three bands (O1–O3) as well as a pellet (O4). Individual bands were removed with a pipette and washed with HB. Finally, pellets were resuspended in HB (final concentration: 1 mg/ml).

A second subcellular centrifugation was performed with fractions O1/O2 or O1 alone. 2.3 ml of the diluted material was loaded onto a pre-equilibrated Percoll step gradient (8, 10, 12, 14, 16 and 20% Percoll in HB, 0.3–0.6 mg/ml total protein loaded). Following centrifugation in a Beckman ultracentrifuge (SW40Ti rotor, 2.6×10^9 ω^2t, 4°C, $32\,500 \times g$), six bands (P1–P6) were observed (see Fig. 1). Fractions were collected, washed with HB, and combined. After a second centrifugation, the resulting pellets were fixed as described below for EM.

2.2. Synaptic stimulation of DS

Fraction O1 was resuspended in aerated Krebs buffer (without Mg^{2+} or Ca^{2+}) to a final protein concentration of 1 mg/ml, warmed to 37°C (5 min), Ca^{2+} (1.4 mM final concentration) added and further incubated (15 min). Stock solutions of glutamate agonists were added to aliquots of fraction O1 to yield (final concentrations): (i) 300 μM L-glutamate containing 10 μM glycine without Mg^{2+}, (ii) 300 μM NMDA containing 10 μM glycine without Mg^{2+} or (iii) aerated Krebs buffer (mock treatment), and incubated (5 min, 37°C). The reaction was stopped by sonication and samples were immediately used or frozen at −20°C.
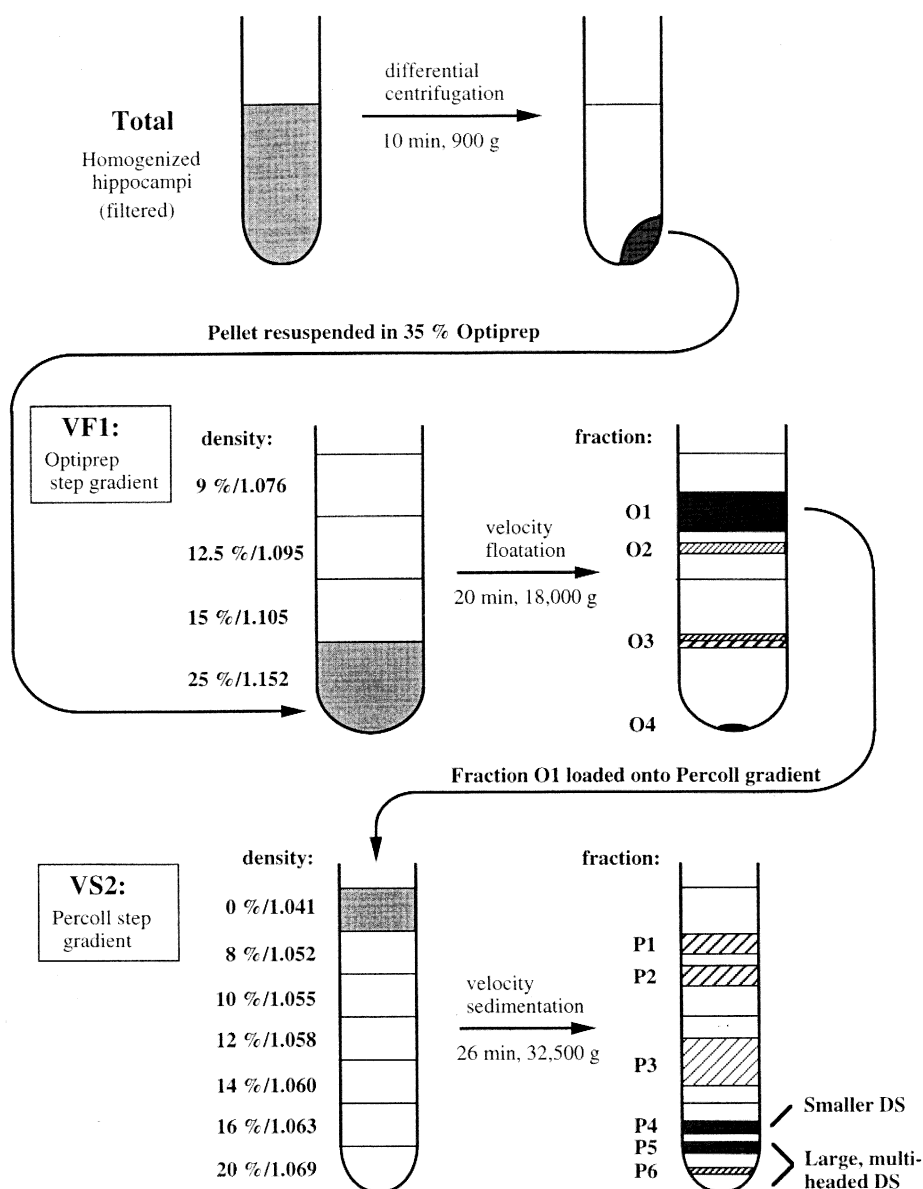
Purification scheme

Fig. 1. Flow diagram for the purification of isolated DS. See text for details. The density unit is g/ml. Abbreviations: VF1, velocity flotation gradient 1; VS2, velocity sedimentation gradient 2; DS, dendritic spines.

2.3. Assay of NOS catalytic activity

The NOS catalytic activity was assayed by measuring the Ca^{2+}-dependent conversion of [^{3}H]arginine to [^{3}H]citrulline as described [12]. The NOS inhibitor $N\omega$-nitro-L-arginine (NNA, Sigma, N-5501, St. Louis, MO, USA) served as a control to determine the background of the reaction.

2.4. Electron microscopy

Individual bands were collected, pelleted in an Eppendorf centrifuge (3 min, 25°C, medium speed) and fixed by overlaying with 1.6% glutaraldehyde, 2.0% paraformaldehyde in 0.1 M Sørenson's phosphate buffer (Electron Microscopy Sciences, Fort Washington, PA, USA). Pellets were processed for Epon embedding according to the method of either Phend et al. [13] or Marsh et al. [14]. Thin sections (100 nm) were prepared on a RMC MT7 or RMC MTX microtome, collected on nickel grids coated with Formvar and carbon (Electron Microscopy Sciences) and post-contrasted with 3% aqueous uranyl acetate and Reynold's lead citrate. Grids were viewed using a JEOL 100CXII or JEOL 1200EXII electron microscope operating at 80 keV.

For the EM quantitation (Table 1), we took 4–8 representative pictures of the respective fractions at 4800× magnification and quantified the selected structures observed per 1250 μm². From these values we estimated enrichment factors for myelin, nuclei and DS (labelled 'Pre/Post'). For the purposes of quantification, only large DS, i.e. spines with diameters greater than 1 μm or spines in association with pre-synaptic terminals greater than 1 μm in diameter, were included in the analysis.

3. Results and discussion

Capitalizing on the published observation that manual homogenization of rat hippocampal tissue yielded intact MF synaptosomes [6,7], we have developed a revised and improved isolation procedure for CA3-DS which are still associated with the MF terminals. The subcellular fractionation is based on two different density gradients, Optiprep and Percoll

(Fig. 1). The aims of this study were first, to deplete for recognizable structures like nuclei, free mitochondria, cell body fragments, broken or intact (red blood) cells, medullated fibers, myelin and small synaptosomes, and second, to enrich for MF terminals and their associated functional DS. The purification progress was monitored by taking electron micrographs from the various fractions.

3.1. Flotation of DS in an Optiprep gradient

To improve fractionation of hippocampal tissue, a $900 \times g$ pellet from a filtered tissue homogenate [6,7] was overlaid with an Optiprep step gradient (Fig. 1). This gradient material has two main advantages: (i) Optiprep allows the isolation of mammalian nuclei since their density in this medium is unusually high (M.P. Rout and G. Blobel, personal communication). (ii) In contrast to the membrane-adhesive Percoll, Optiprep enables organelle fractionation based more heavily on the properties of the tissue itself. A second important modification is the flotation of material instead of sedimentation, yielding a good separation of the high density structures in the homogenate starting material (see Fig. 1). This led to the appearance of three bands (O1–O3) and a pellet (O4). The first densely white, voluminous band (O1) appeared at the interface of 9 and 12.5% Optiprep, the second very fine band (O2) appeared at the interface of 12.5 and 15% Optiprep close to the first band, and the third brownish band (O3) was found at the interface of 15 and 25% Optiprep. Bands O1/O2, O3 and the pellet (O4) were collected and evaluated for the presence of nuclei (DAPI staining, fluorescence microscopy) (Fig. 2A–C) and overall morphology (transmission EM) (Fig. 2D–F). Almost all the DAPI staining was observed in band O3 and the pellet O4 (Fig. 2B,C) consistent with the observation that the density of nuclei exceeds that of 25% Optiprep (M.P. Rout and G. Blobel, personal communication). In contrast, the first Optiprep fraction (band O1/O2) only contained minor DAPI staining (Fig. 2A) representing free mitochondria rather than nuclei.

3.2. EM analysis of fractions from the Optiprep gradient

At the ultrastructural level, the lightest fraction (band O1/O2) consisted of large MF synaptosomes with various DS attached (Fig. 2D) as well as smaller synaptic profiles, myelin, and free mitochondria. However, few nuclei, fibers, cell body fragments or intact cells were seen in this fraction. The third band O3 contained intact nuclei, free mitochondria and even some intact cells including red blood cells and endothelial cells

(Fig. 2E). The pellet O4 (Fig. 2F) represented almost pure intact nuclei. In conclusion, we found that the CA3-DS associated with the MF terminals float to the 9%/12.5% Optiprep interface whereas nuclei and broken or intact cells remain mostly at the bottom of the gradient.

To further characterize the material in the upper two bands (O1/O2), these were collected separately, fixed and embedded for EM analysis (Fig. 3). We found the easily identifiable MF terminals with their complex DS enriched in the prominent band O1. Compared to the ultrastructural morphology of DS found in vivo [15], they appear very similar to our isolated DS suggesting that both the pre-synaptic terminal and the post-synaptic DS might still be intact and their membranes resealed. The DS often contained PSD, mitochondria, endocytic tubular and vesicular structures, polyribosomes (PR) and a typical membrane structure called spine apparatus (SA) (Fig. 3A,B).

In contrast to band O1, the less prominent band O2 contained significantly fewer MF-derived CA3-DS. Instead, large complex structures were observed representing small pre-synaptic terminals contacting the shaft of dendritic fragments (Fig. 3C,D). One particularly interesting example is depicted in Fig. 3C where a complex dendritic structure intercalates into a MF terminal. The dendritic shaft containing a SA at the neck yields into a small DS. Both the dendritic shaft and its attached DS are in the same plane of the section and are in contact with the MF terminal. When we analyzed these dendritic fragments in more detail, we found that they contain a rich ultrastructure including endocytic tubulo-vesicular structures, mitochondria, and multivesicular bodies (Fig. 3D).

3.3. Sedimentation of DS in a Percoll gradient

To further purify the observed DS, we loaded the Optiprep bands O1/O2 on a Percoll step gradient (8, 10, 12, 14, 16 and 20% Percoll). The resulting centrifugation (see Fig. 1) yielded in the separation of six bands (P1–P6): a close double band at the interface of 0 and 8% Percoll (P1, P2), a smear at the interface of 12 and 14% Percoll (P3), a second double band at the interface of 16 and 20% Percoll (P4, P5) and a final band in 20% Percoll (P6). Samples of all bands were again examined with the electron microscope (Fig. 4, data not shown). Bands P1, P2 and P3 mainly consisted of myelin and cell fragments (data not shown). Band P3 additionally contained some other small structures, but no large synaptoneurosomes (data not shown). Fraction P4 contained large dendrites with attached synaptic boutons (Fig. 4A) and small

Table 1
Purification table

Fraction	Myelin	Change	Nuclei	Change	Pre/Post[a]	Change
H	39	–	2	–	4 (2)[b]	–
P$_1$-pellet[c]	23	0.59	7	3.5	7 (4)	1.8 (2)[d]
O1/O2	16	0.41	1	0.5	10 (5)	2.5 (2.5)
P4	16	0.41	2	1.0	19 (7)	4.8 (3.5)
P5	12	0.31	0	–	17 (5)	4.3 (2.5)
P6	10	0.26	2	1.0	21 (15)	5.3 (7.5)

Depletion of myelin and nuclei and enrichment for DS is based on the number of structures per area (1250 μm^2) in respective electron micrographs from the resulting fractions depicted in Fig. 1. 'Change' indicates fold change over homogenate.
[a]Large 'Pre/Post' indicates intact pre- and post-synaptic pairs defined by the presence of pre- and post-synaptic densities with at least one member of the pair having a diameter greater than 1 μm.
[b]Number of 'Pre/Post' identified as MF synapses shown in parentheses.
[c]P$_1$-pellet is the first low speed nuclear pellet ($900 \times g$), see Fig. 1 for details.
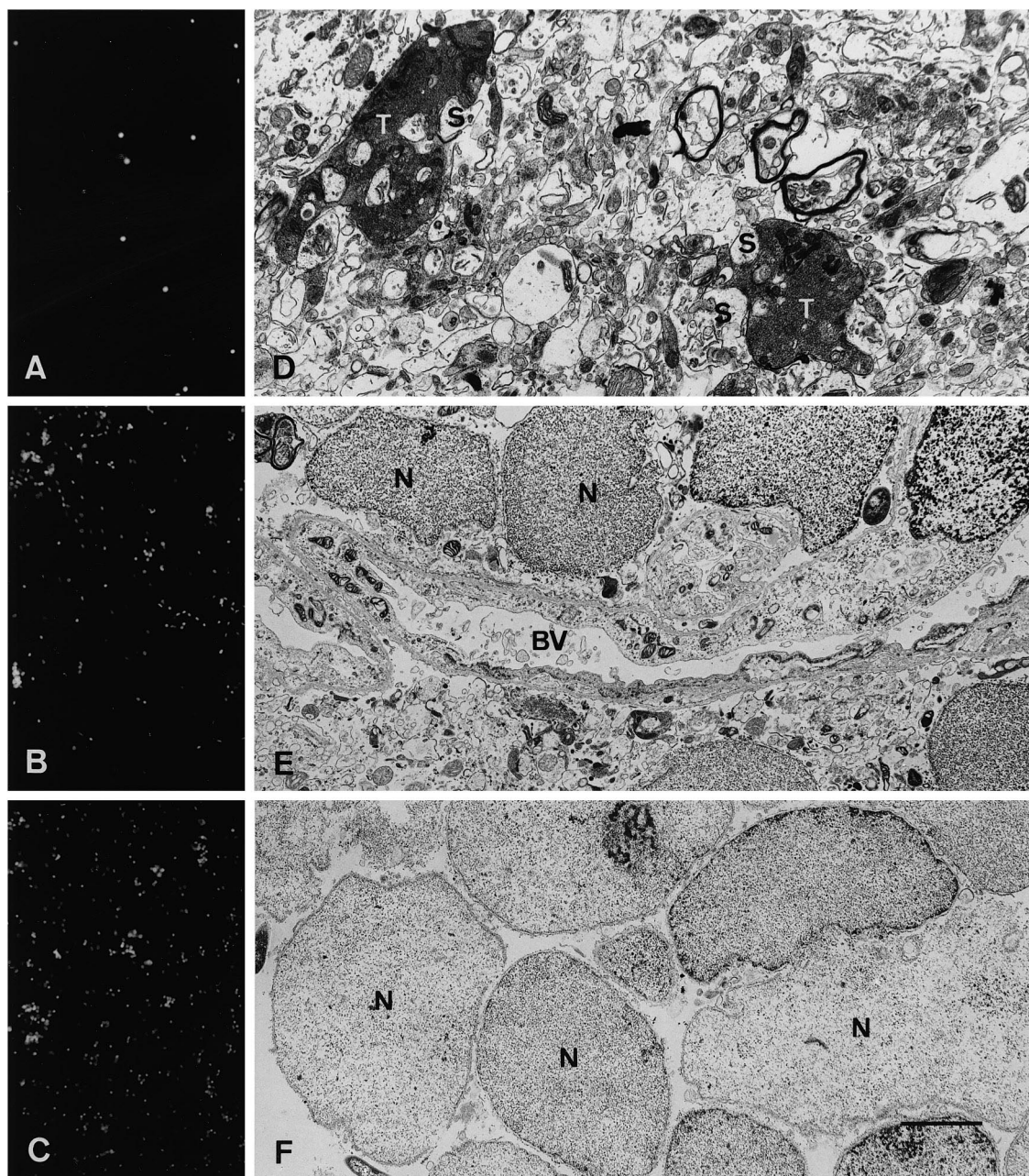[d]Fold change over homogenate for MF synapses shown in parentheses.

Fig. 2. Characterization of Optiprep fractions O1–O4 by fluorescence microscopy (DAPI staining) and transmission electron microscopy. The left panels represent the DAPI staining to account for nuclear (and mitochondrial) contaminations: the right panels represent the respective electron micrographs showing the overall morphology of the three fractions. A,D: Fraction O1/O2 consisting of large MF terminals (T) in contact with various DS (labeled 'S'); B,E: Fraction O3 containing isolated nuclei (N), and some intact red blood cells and endothelial cells coming from blood vessels (BV); C,F: Pellet O4 of the Optiprep gradient containing intact nuclei. Bars: A = 1.4 μm, B = 1.9 μm, C = 2.0 μm.

pre- and post-synaptic pairs (Fig. 4B) in addition to cell fragments. Clearly defined terminals and spines comprised 5–15% of the pellet volume. Fraction P5 contained large MF synaptic contacts that often included complexes of multiple spines with a single terminal (Fig. 4C,D). MF terminals and associated DS comprised 10–25% of the pellet volume. Nuclei, however, were clearly depleted in this fraction. The highest density fraction (P6) contained very large, dense MF terminals that included large mitochondria and multiple contacts with DS (Fig. 4E,F). These structures accounted for 5–15% of the pellet volume. The P6 fraction also had a low level of nuclear contamination. DS, especially those associated with MF ter-

minals, often contained a SA and multiple post-synaptic densities.

3.4. Enrichment of DS based on ultrastructure

The purification procedure succeeded in decreasing the amount of contamination by myelinated fibers 2.5-fold (see Section 2.4 for details) in the O1/O2 fraction and 4-fold in the P6 fraction, relative to the initial homogenate (Table 1). Nuclear contamination in the O1/O2 fraction was decreased by a factor of two relative to the homogenate, whereas the P6 fraction was comparable to the homogenate. However, compared to the initial low speed pellet (P_1-pellet), both the O1/

O2 and P6 fractions showed a significant decrease in nuclear contamination, at 7-fold and 3.5-fold, respectively. The comparison to the low speed nuclear pellet is relevant in that it represents a concentration step for large, dense structures including nuclei and MF nerve endings, a step common to similar protocols for purifying MF terminals [6,7]. More importantly, however, intact pre- and post-synaptic pairs (labelled 'Pre/Post' in Table 1) were significantly concentrated in the O1/O2 fraction and the Percoll fractions P4–P6, with a 2.5- and 5.3-fold enrichment relative to the nuclear pellet, respectively. If one compares these values to the depletion of myelin and nuclei, then DS are 5.0-fold enriched over nuclei and 6.1-fold over myelin in the O1/O2 fraction, and 4.8–5.3-fold enriched over nuclei and 11.7–20.4-fold over myelin in the respective Percoll fractions. These observed structures included (i) large DS with multiple small pre-synaptic terminals, (ii) single, large pre-synaptic terminals paired with single, large DS, and (iii) classical MF terminals with densely packed synaptic vesicles, and multiple, engulfed DS. The MF synapses

were particularly enriched in the P6 fraction where the structures were enriched 7.5-fold compared to nuclei or 28.9-fold to myelin. Fractions O1/O2 and P4–P6 also contained a large number of small synaptic terminals, often paired with post-synaptic DS. These structures were not enumerated since the pre- and post-synaptic densities were rarely visible to confirm the presence of synaptic contacts. However, aggregation of synaptic vesicles suggested the presence of synaptic contacts.

The goal of this study was to devise a purification scheme for the enrichment of functional DS derived from hippocampal neurons. A protocol describing MF boutons of dentate granule cells still associated with CA3-DS served as a starting point [6]. We performed a morphological and functional characterization of the post-synaptic structures and introduced several important modifications leading to a fraction containing a high percentage of large multi-headed DS still attached to MF terminals (see Table 1 and results). The ultrastructure of the DS was very reminiscent to that of intact hippocampal neurons in vivo [15–17]: the isolated DS often contained PSD,
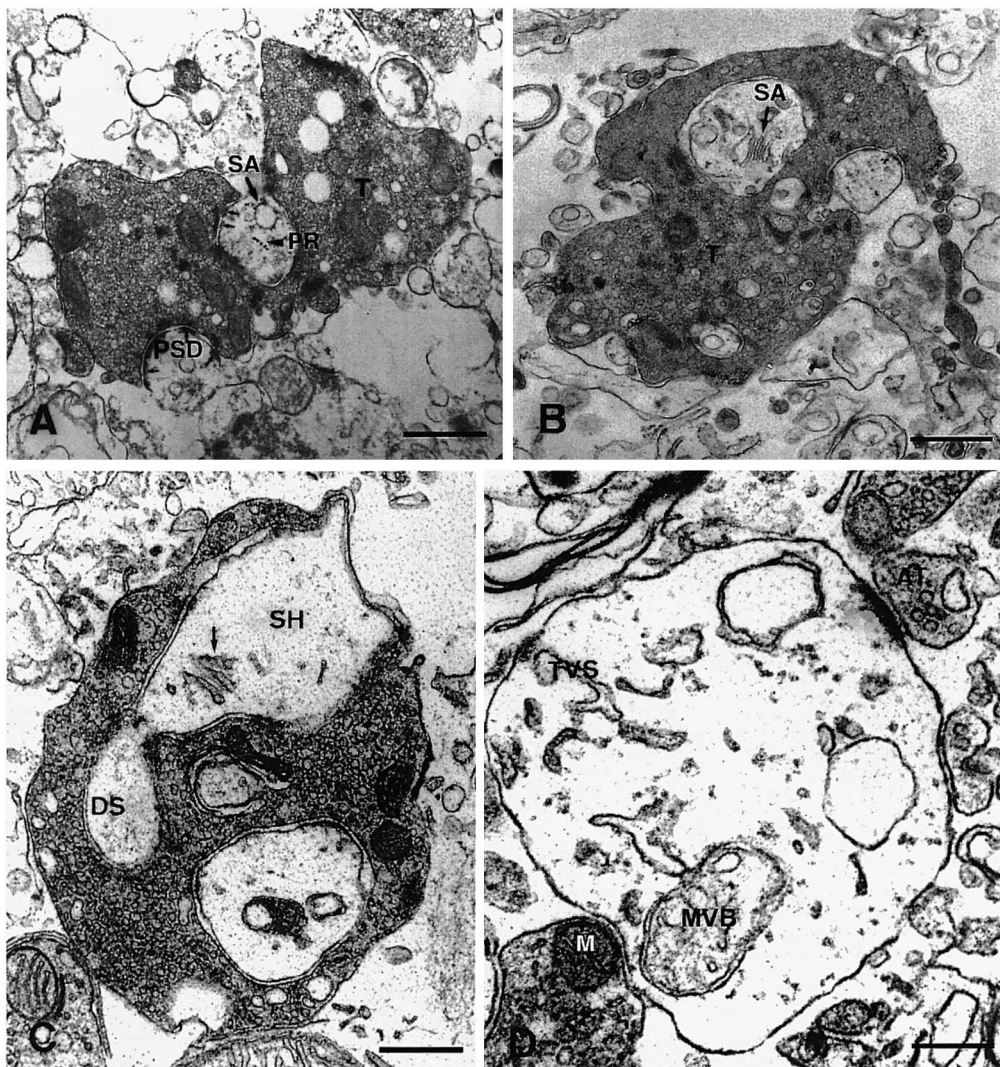

Fig. 3. High magnification electron micrographs of isolated DS from Optiprep fraction O1 (A,B) and O2 (C,D). A: DS with PSD (small arrows), PR (arrowhead) and a (swollen) SA (large arrow), in contact with a presynaptic terminal (T). B: DS with a SA (large arrow). C: A large MF terminal with two DS and a dendritic shaft (DSH) with a protruding dendritic spine (DSP). The SA (arrow) is found near the neck of the dendritic spine. D: Small functional synapse (AT) contacting a large dendritic shaft containing a PSD, tubulo-vesicular structures (TVS), a multivesicular body (MVB) and mitochondria (M). Bar, A = 500 nm, B = 450 nm, C = 400 nm, D = 225 nm.
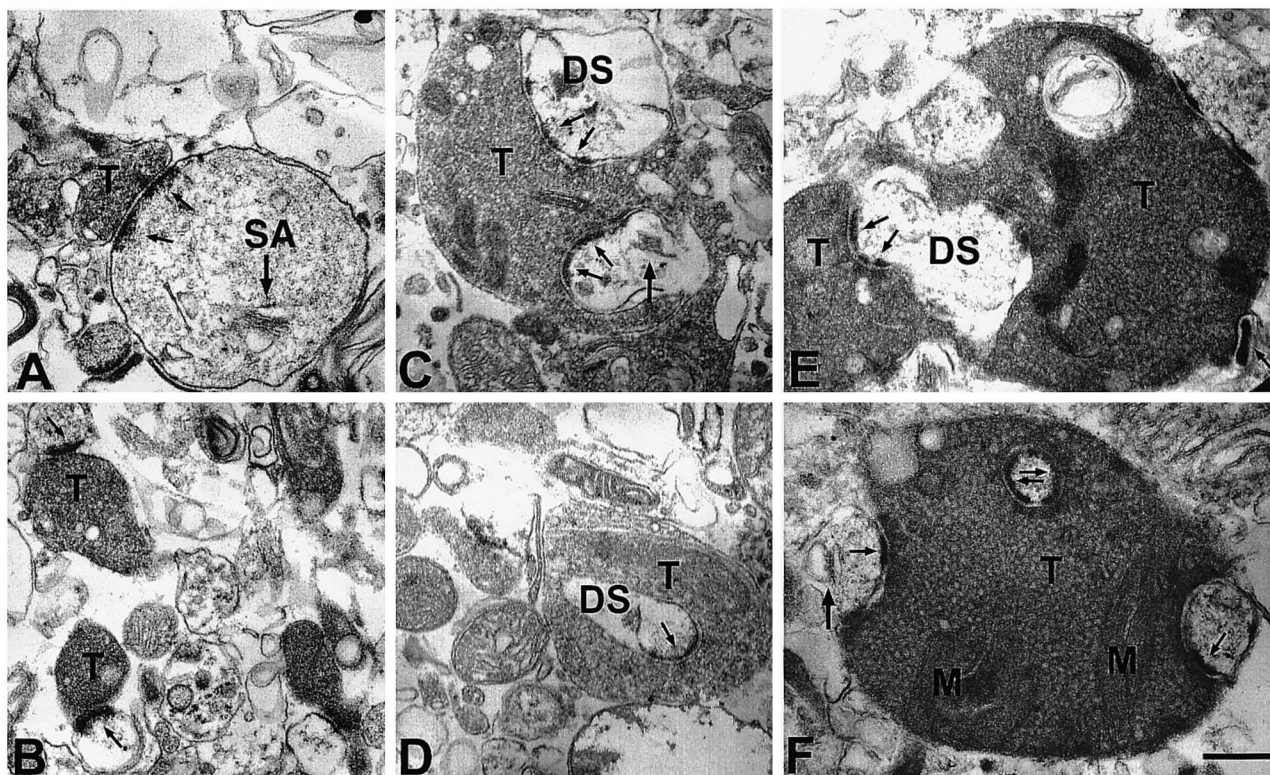
Fig. 4. Electron micrographs of material isolated from the second Percoll gradient (fraction P4–P6). A,B: Fraction P4 consists of both large dendrites with evident PSDs (small arrows), a SA (large arrow) and a small attached synaptic bouton (T), as well as small pre- and post-synaptic pairs; C,D: Fraction P5 of large MF terminals (T) in contact with complex DS containing PSDs (small arrows) and a SA (large arrow); E,F: Fraction P6 shows very large, dense MF terminals with mitochondria (M) and DS containing a SA (large arrow). Bar, 300 nm.
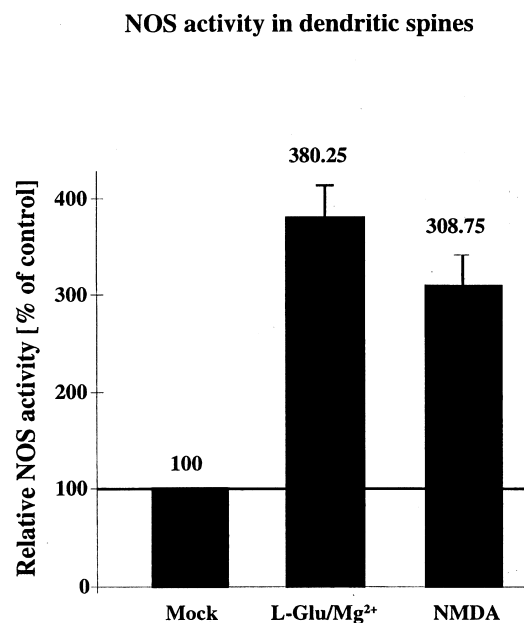
NOS activity in dendritic spines

Fig. 5. NOS activity in CA3-DS upon stimulation with glutamate agonists. Isolated DS (fraction O1/O2) were either treated with 300 μM L-glutamate, NMDA or mock-treated. NOS activity was assayed by measuring the Ca^{2+}-dependent conversion of [³H]arginine to [³H]citrulline [12] and the relative NOS activity is shown as percentage of the mock-treated control. Error bars indicate the standard errors of the mean ($\pm$S.E.M.): 31.7 for L-Glu/Mg^{2+}, 31.1 for NMDA.

mitochondria, endocytic tubular and vesicular structures, polyribosomes and typical membrane structures called 'spine apparatus' (Fig. 3, see below).

What enzymes might be suitable for a functional assay to probe for the integrity of dendritic fragments or DS? Recent data suggested that nitric oxide (NO), a gas molecule produced by the enzyme NOS, is synthesized post-synaptically following synaptic activation [12,18]. Therefore, we performed a set of pilot experiments in which we explored whether NOS might serve as such a functional marker and whether the observed NOS activity can be stimulated in DS by local calcium influx through glutamate receptors. When fraction O1 containing DS was exposed to glutamate receptor agonists, e.g. NMDA, glutamate- or mock-treated, a consistent 3–4-fold activation of NOS was observed (Fig. 5). This is in good accordance with values observed for brain slices [19] indicating that isolated DS are metabolically active.

Interestingly, all three isoforms of NOS, the constitutive endothelial and neuronal isoforms as well as an inducible macrophage nitric oxide synthase [20] have been found to be expressed in the hippocampus in vivo and/or in hippocampal dendrites in vitro ([21,22], M. Kiebler and I. Hemraj, unpublished observations but also see [23]). We therefore like to propose that the stimulatable NOS activity might serve as a post-synaptic marker enzyme to assay for the functional integrity of DS. The local calcium influx through the glutamate receptors would thereby activate the post-synaptically located NOS and lead to the formation of NO which then can be easily detected by well established enzyme assays [12,18]. This in turn would indicate that the biochemical path-

ways following post-synaptic neurotransmitter receptor activation remain intact.

In conclusion, we anticipate that this new experimental post-synaptic system will be useful in the study of various aspects of post-synaptic functions at the biochemical and molecular level thereby having a similar impact on the molecular characterization of pre-synaptic boutons as the synaptosomal preparation had two decades ago.

References

[1] Crick, F. (1982) Trends Neurosci. 5, 44–46.
[2] Whittaker, V. (1964) Biochem. J. 90, 293–303.
[3] Israël, M. and Whittaker, V. (1965) Experientia 21, 325–326.
[4] Daly, J.W., McNeal, E.T., Partington, C., Neuwirth, M. and Creveling, C.R. (1980) J. Neurochem. 35, 326–347.
[5] Hollingworth, E.B., McNeil, E.T., Burton, J.L., Williams, R.W., Daly, J.W. and Creveling, C.R. (1985) J. Neurosci. 5, 2240–2253.
[6] Terrian, D.M., Johnston, D., Claiborne, B.J., Ansah-Yiadom, R., Strittmatter, W.J. and Rea, M.A. (1988) Brain Res. Bull. 21, 343–351.
[7] Taupin, P., Zini, S., Cesselin, F., Ben-Ari, Y. and Roisin, M.-P. (1994) J. Neurochem. 62, 1586–1595.
[8] Rao, A. and Steward, O. (1991) J. Neurosci. 11, 2881–2895.
[9] Chicurel, M.A., Terrian, D.M. and Potter, H. (1993) J. Neurosci. 13, 4054–4063.
[10] Weiler, I. and Greenough, W. (1991) Mol. Cell. Neurosci. 2, 305–314.
[11] Weiler, I. and Greenough, W. (1993) Proc. Natl. Acad. Sci. USA 90, 7168–7171.
[12] Son, H., Hawkins, R.D., Martin, K., Kiebler, M., Huang, P.L., Fishman, M.C. and Kandel, E.R. (1996) Cell 87, 1015–1023.
[13] Phend, K.D., Rustioni, A. and Weinberg, R.J. (1995) J. Histochem. Cytochem. 43, 283–292.
[14] Marsh, E.W., Leopold, P.L., Jones, N.L. and Maxfield, F.R. (1995) J. Cell Biol. 129, 1509–1522.
[15] Peters, A., Palay, S. and Webster, H. deF. (1991) The Fine Structure of the Nervous System. Neurons and their Supporting Cells, 3rd edn., Oxford University Press, Oxford.
[16] Chicurel, M.A. and Harris, K.M. (1992) J. Comp. Neurol. 8, 169–182.
[17] Boyer, C., Schikorski, T. and Stevens, C.F. (1998) J. Neurosci. 18, 5294–5300.
[18] Arancio, O., Kiebler, M., Lee, C.J., Lev-Ram, V., Tsien, R.Y., Kandel, E.R. and Hawkins, R.D. (1996) Cell 87, 1025–1035.
[19] Bredt, D.S. and Snyder, S.H. (1989) Proc. Natl. Acad. Sci. USA 86, 1030–1033.
[20] Knowles, R.G. and Moncada, S. (1994) Biochem. J. 298, 249–258.
[21] Dinerman, J.L., Dawson, T.M., Schell, M.J., Snowman, A. and Snyder, S.H. (1994) Proc. Natl. Acad. Sci. USA 91, 4214–4218.
[22] Wendland, B., Schweizer, F.E., Ryan, T.A., Nakane, M., Murad, F., Scheller, R.H. and Tsien, R.W. (1994) Proc. Natl. Acad. Sci. USA 91, 2151–2155.
[23] Huang, E.P. (1997) Curr. Biol. 7, R141–143.